STATIC AND SEISMIC BEHAVIOUR OF EMBEDDED ANCIENT VAULTS

A. Leontari[1], N. Makris[2], M. Apostolou[3] and G. Gazetas[4]

[1]Dr, National Technical University of Athens, Greece, airinaleo@gmail.com

[2]Professor, South Methodist University, Dallas, USA, nmakris@smu.edu

[3]Dr, National Technical University of Athens, Greece: m_apostolou@hotmail.com

[4]Emeritus Professor, National Technical University of Athens, gazetas@central.ntua.gr

ABSTRACT

The role of soil-structure interaction in the behaviour of masonry vaulted structures is investigated. Nonlinear analyses are carried out using finite element modelling. The influence of the surrounding soil and the structure geometry on a partially or fully embedded vault subjected to static loading is unveiled. An interesting finding is the development of two arching mechanisms through which the structure attains static equilibrium. Dynamically, a fully embedded vault is subjected to idealised Ricker pulses and the interplay between soil, structure, and excitation characteristics is highlighted. Results are obtained for acceleration distributions at the soil stratum and dynamic earth pressures on the structure and the excavation surface.

Keywords: Ancient Vaults, Seismic behaviour, soil-structure interaction, FE Method, Stability, geo-structure

INTRODUCTION

Embedded Ancient Vaults are masonry *geostructures* in which either the pair of buttresses alone or the entire structure are covered with soil. The backfill soil is retained by the structure, especially by the two buttresses and, in fully embedment cases, it imposes to the structure overburden pressures. Two prominent examples of such monumental masonry *geostructures* are illustrated in Figure 1. The paper performs nonlinear analyses for the static and earthquake loading using Finite Elements. The response of the structure is governed primarily by the response of the soil. Depending on pressures applied by the backfill or overburden soil different deformation modes of the vaulted structure are mobilised. Static results are presented in the form of contours of structural displacements on x and y components during successive stages of construction.

Dynamically the system is excited with several Ricker wavelets as base excitations. The seismic response is a complex soil-structure interaction problem. Structure movements and dynamic earth pressures depend on the response of the underlying soil, as well as the response of the backfill, the inertial and flexural responses of the buttresses, and the nature of the input motions. Acceleration distributions at three different selected sections further illustrate the response to increasing excitation levels PGA = 0.2 g ~ 1 g. For each loading case the maximum and minimum dynamic earth pressures in the backfill-buttress interface are obtained. For Ricker pulses of dominant period T_E = 0.90 *s,* intense soil reactions occur in the arch-buttress interface, suggesting the tendency of the arch to flatten. The evolution of the lateral stresses that develop along the left excavation boundary when Ricker wavelets of three different dominant periods (T_E = 0.6 s, 0.90 s, 1.33 s) are applied helps to visualise the most vulnerable locations of the vault.

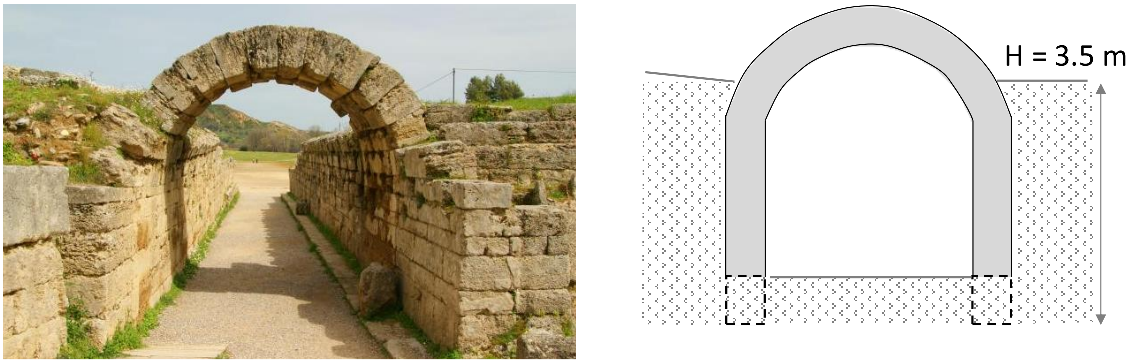

(a)Type I embedded vaulted structures

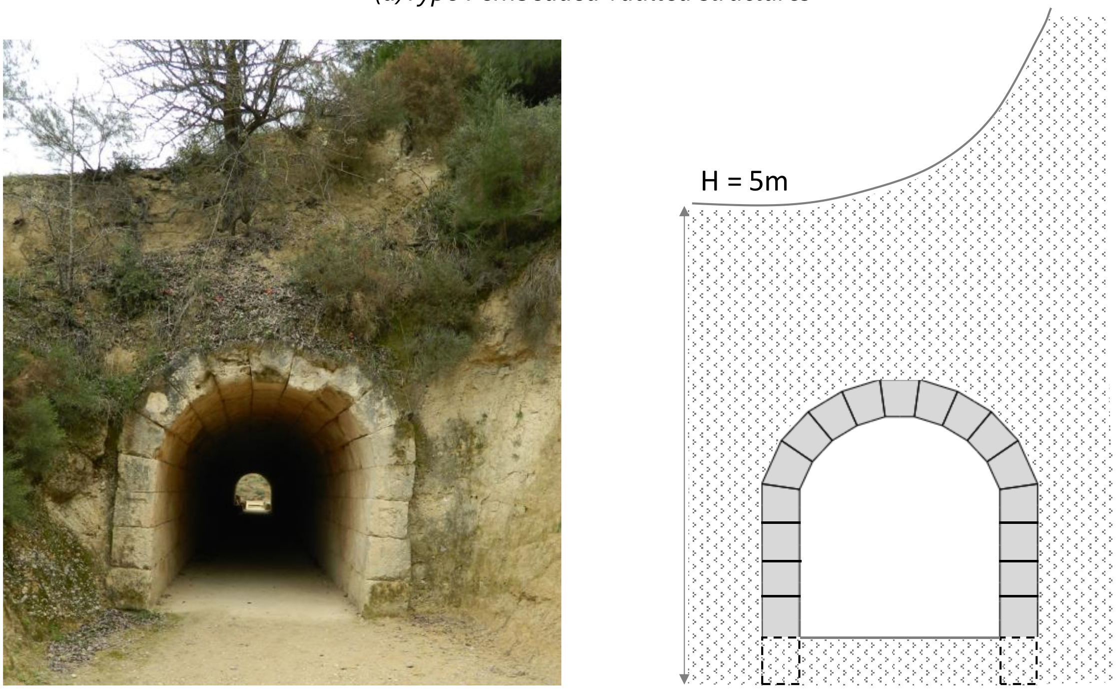

(b)Type II embedded vaulted structures

Figure 1. *Embedded vaulted structures in Ancient Greece: (a) masonry vault with embedded lateral walls, used as the entrance to the ancient stadium of Olympia, (b) masonry vaulted tunnel, used as the entrance to the ancient stadium of Nemea.*

FINITE ELEMENT MODELLING

Two-dimensional configuration

Nonlinear analysis of the response under static and earthquake loading is implemented numerically with the Finite Element Method. To this extent, the sophisticated code ABAQUS is utilised. Figure 2 portrays the finite element discretisation of the model along with a schematic layout of modelling details. A masonry vaulted structure consisting of a finite number of voussoirs is constructed in a trench at a depth of 5.50 m which is excavated in cohesive soil. The structure and the surrounding soil are represented with plane-strain elements. For the purposes of the two-dimensional modelling, soil medium is represented with quadrilateral, continuum elements. Regarding the finite element mesh, a sufficiently refined one is required especially in the area around the structure to ensure the adequacy of the results from the Abaqus simulation. A fairly fine mesh is selected for an area of 30 m length and 15 m height where the magnitude of stresses is of high interest. It is meshed with quadrilateral plane strain continuum elements of 0.25 m x 0.20 m (detail a). Towards lateral boundaries the mesh is coarser with quadrilateral elements of 0.50 m x 0.20 m (detail b). The material properties of the structure include a modulus of Elasticity E= 6.5 GPa, a Poisson's ratio of 0.25, and density of 2.2 t/m^3. Regarding lateral boundaries, the corresponding nodes at the opposite vertical sides of the same elevation are tied together and forced to move simultaneously only in the horizontal direction preventing any rotation. The side nodes of the excavation are also constrained, as temporary retaining scheme to avoid ground movements. Vertical component of the displacement is constrained along the base of the soil medium (vertical movement of the base is restricted). A sophisticated contact algorithm is utilised for modeling contact interface at hinges sections [voussoir-to-voussoir and voussoir-to-buttress (monolithic)] as well as at soil-structure interface. A sufficiently large coefficient of friction (μ = 0.7) was chosen to approach pure rocking conditions associated with slender systems. The effect of sliding on the response is negligible. Material damping is also neglected. A soil profile of homogeneous cohesive soil in which stiffness and strength are gradually increasing with depth is implented in this study. The elastoplastic soil behavior of cohesive soils under undrained conditions is described with Von-Mises failure criterion, available in the finite element code Abaqus.

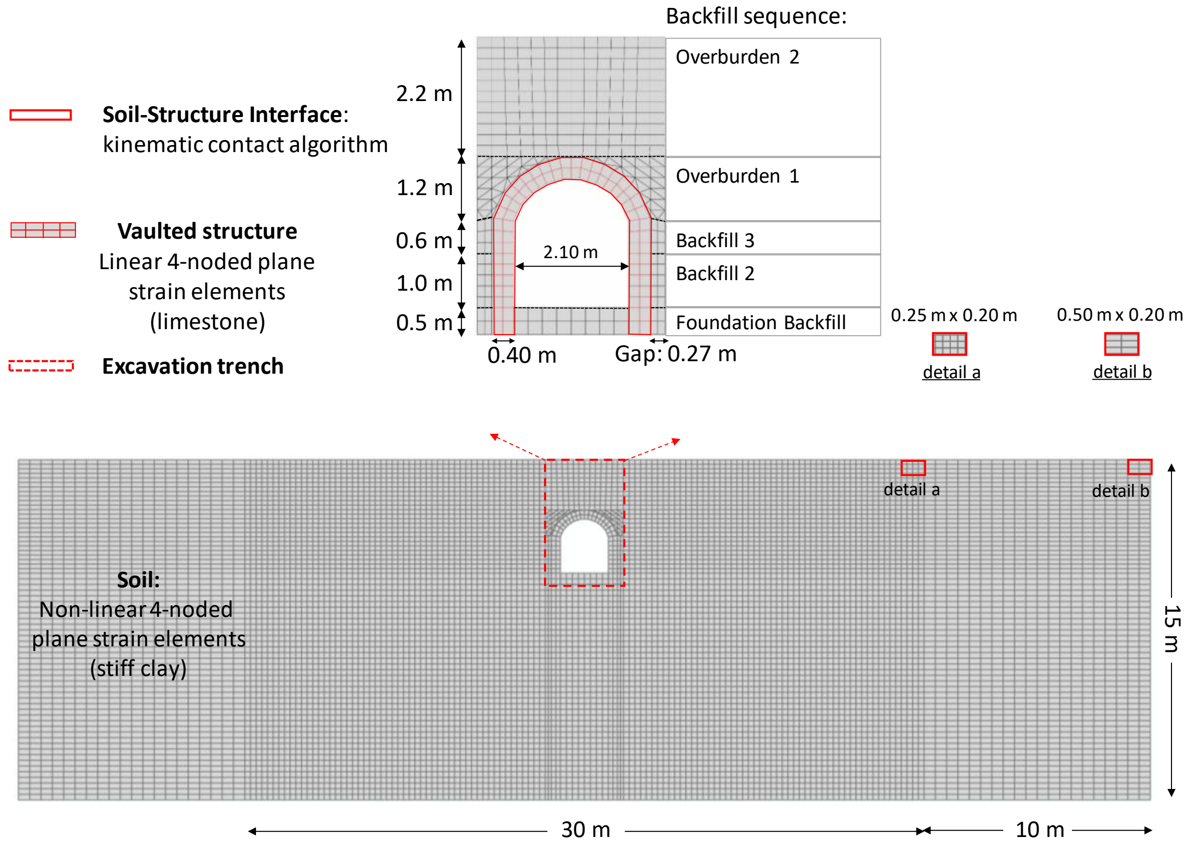

Figure 2. *The excavation trench, the masonry vaulted structure, and details of the backfill and overburden layers; geometry and finite element discretisation assuming plane strain conditions.*

HORIZONTAL AND VERTICAL DISPLACEMENTS

Figure 3 illustrates the contours of structural displacements on x and y components due to the successive embankment of the structure. The response of the structure is governed primarily by the response of the soil adjacent to the structure. The changing forces from the backfill or overburden soil that are applied to the vaulted structure mobilise different deformation modes. The magnitude of these displacements depends on: a) the structure geometry, b) the masonry stiffness, c) the soil stiffness and, d) the construction sequence. For the sake of convenience, displacements are positive when they are directed along the positive direction of the corresponding co-ordinate axis. Three essential phases of the structure's embankment are distinguished: (i) the buttresses are fully backfilled (the soil arises at the height of h_3 = 2.16 m from the foundation base), (ii) the arch is covered to its crown (h_4 =3.30 m) and (iii) the placement of overburden soil above the arch forms the final soil surface at a height of h_5 =5 m from the foundation base.

Upon completion of backfill, the compliance of the buttress is fully mobilised as depicted in Figure 3i. These inwards translational and rotational displacements of each buttress (horizontal displacement of 0.4 mm) are restrained by the arch as severe friction forces are developed along each buttress-to-arch interface. Static equilibrium at the end of this phase is established resulting in contact forces which are reduced along the buttress and increased along the arch (tendency for active and passive state respectively). As backfill proceeds and the arch is covered with soil up to its top point (Figure 3ii), soil contact forces impose bending of the arch accompanied with inward horizontal displacements as well as upward movement especially of its central voussoirs (1.8 mm approximately). Eventually, when the excavation is fully recovered with soil, the crown is gradually depressed and the overburden pressures restore the undeformed geometry.

Static equilibrium is then established as the overburden load is undertaken through two arching mechanisms: by the structural arch and by soil arching. In the first case, the voussoirs are stressed with predominantly axial compression and severe horizontal forces are developed at the arch supports to ensure arching mechanism. These forces are transmitted to the soil medium around these supports which are demonstrated as concentration of the contact pressures. In the second case, the latter mechanism is developed at the back and above the arch and allows of stress paths to divert the structural arch transmitting a part of the overburden load directly to soil medium.

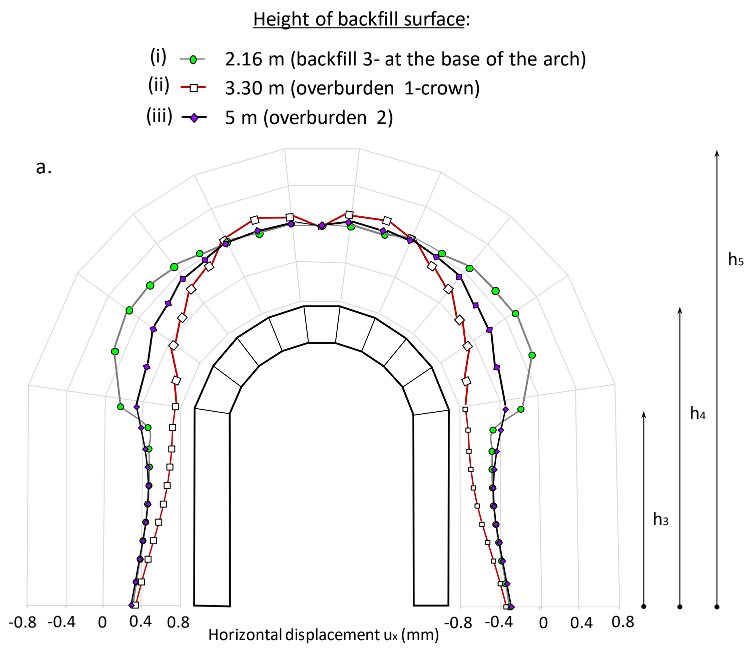

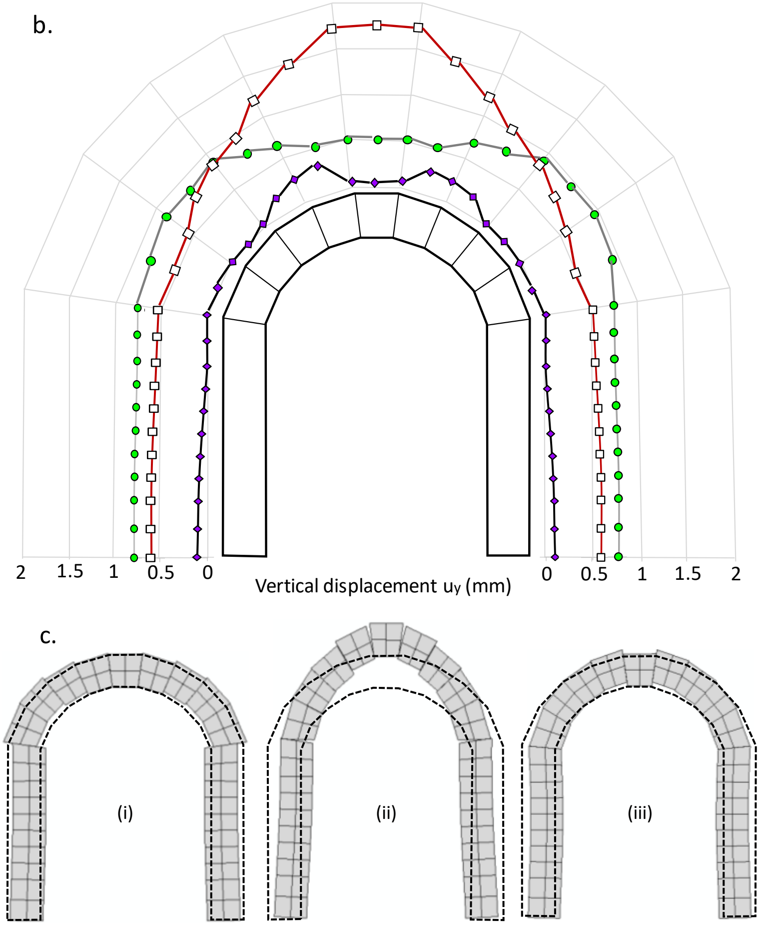

Figure 3. *Contours of (a) horizontal u_x and (b) vertical displacements u_y, (c) deformation mode with a scale factor of 200% of the structure calculated for three different loading increments: (i) the buttresses are fully backfilled to the height of h_3 =2.16 m; (ii) the backfill arises up to the crown, h_4 =3.30 m; and (iii) overburden is placed above the arch, h_5 =5 m from the foundation base.*

SEISMIC RESPONSE

Determining the response of the vault to seismic loading has been a challenging task in the study. Initially, the role of soil amplification will be examined. In this context, the soil base is dynamically excited using idealised excitations. The selected wavelets are characterised by moderate (0.4g) and strong (1g) intensity and two different periods T_E (0.90 & 1.33 s). The acceleration distributions developed to three different selected sections, the one at the centerline of excavation (a: x = 0 m), the second behind the excavation (b: x = 0.25 m) and the third at the far field (c: x = 25 m) will be presented in Figure 4. The most important observations are:

- Shakings of the same acceleration amplitude a_p give similar acceleration distributions throughout each section.
- In moderate shaking of acceleration amplitude of a_p = 0.4 g, the three distributions of maximum acceleration corresponding to different positions in the soil are identical. The explanation for this observation lies on the fact that the soil-structure interface follows the shear deformation of the soil strata.
- The increase of the pulse excitation period from T_E = 0.90 s to 1.33 s seems to have negligible effect on the acceleration distribution.
- Interestingly, the maximum accelerations developed above the structure (z =2.8 m to 5 m) at cases (i) and (iii) remain constant, while in cases (ii) and (iv) deviate significantly from the distribution “route”. The presence of the structure tends to reinforce certain harmonic components of the incident seismic waves. The soil amplification phenomenon is observable from the level of the structure foundation to the surface. It is amplitude dependent and roughly corelated to pulse frequency.
- The sharp peak of the maximum acceleration at the base is due to the soil plastification.

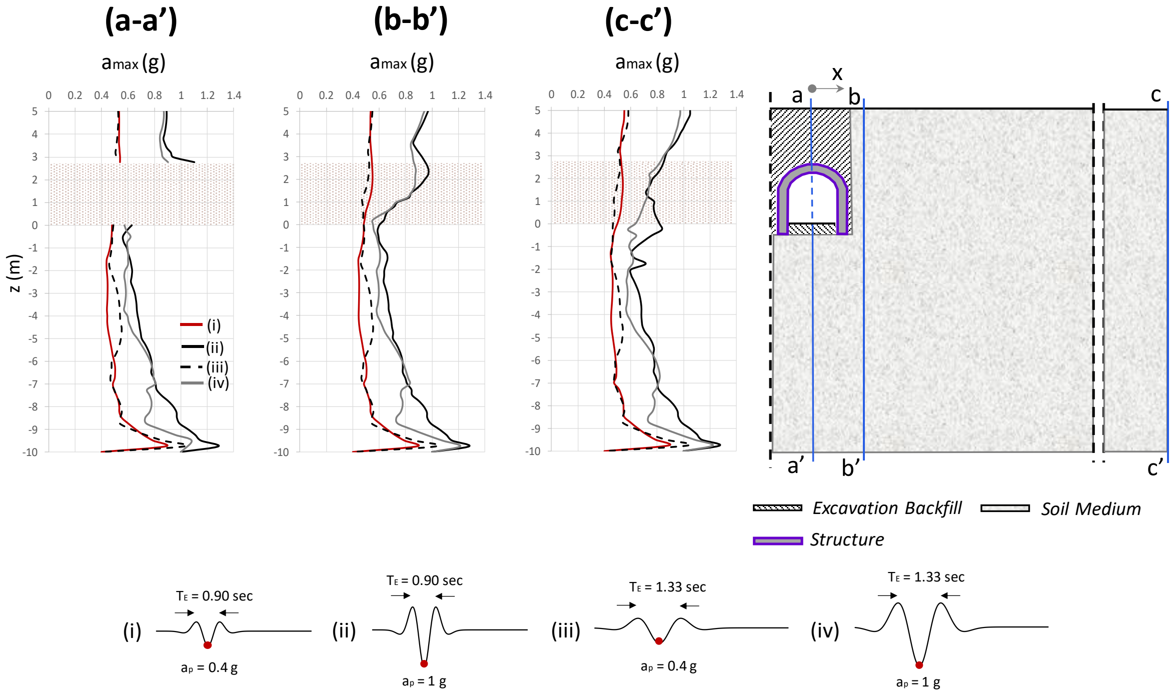

Figure 4. *Distribution of maximum horizontal acceleration along sections a, b and c when the bedrock level is triggered with Ricker pulses: (i) a_p = 0.4 g, T_E = 0.90 ; (ii) a_p =1 g, T_E = 0.90 s; (iii) a_p = 0.4 g, T_E = 1.33 s; and (iv) a_p =1 g, T_E = 1.33 s.*

Horizontal earth pressures

Increasing acceleration levels from weak to very strong intensity has been implemented in the analysis (PGA= a_p = 0.2 *g* ÷ 1 *g*). For each loading case the maximum and minimum dynamic earth pressures in the backfill-buttress interface are computed. For Ricker pulses of period T_E = 0 s (Figure 5), intense soil reactions are observed at the arch-buttress interface, suggesting the crucial demand of the arch to flatten.

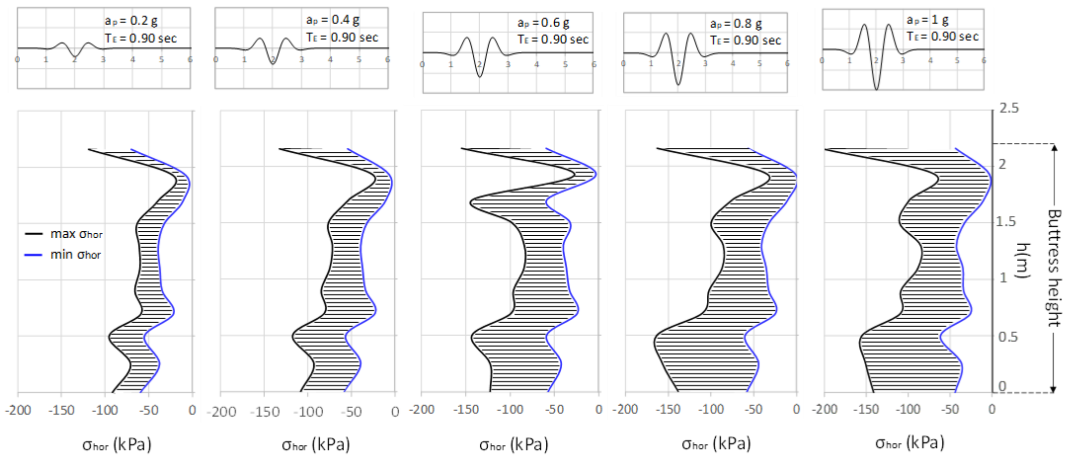

Figure 5. *Illustration of the maximum and minimum dynamic earth pressures in the backfill-buttress interface when the base is subjected to Ricker wavelets of fixed duration T_E = 0.90 s and increasing acceleration amplitude from a_p = 0.2 g to 1 g.*

Next, the relieving role of the backfill to the surrounding soil is examined. The evolution of the lateral stresses that develop along the left excavation boundary when Ricker wavelets of three different durations (T_E = 0.6 s, 0.90 s & 1.33 s) are applied at the base is calculated. For each duration the structure is subjected to a wide range of acceleration amplitudes a_p from very low values (0.2 *g*) to moderate (0.4 *g*, 0.6 *g*) and to very strong (1 *g*). The distribution of the lateral stresses under static condition is used as a yardstick for the comprehension of the effect of the pulse characteristics (a_p, T_E). In the view of the calculated results obtained from the numerical analyses, depicted in Figure 6 it is clear that:

- the predominant period of Ricker pulses does not seem to affect the horizontal earth pressures that develop beyond the backfill soil.
- The earth pressure distribution at the level of the overburden soil (*h* = 2.8 m ÷ 5 m) is linear regardless the pulse characteristics (a_p, T_E).
- The arch mechanism influences the surrounding soil increasing the pressures locally at *h* = 1.66 m.
- There is a notable increase in the lateral earth pressures when larger acceleration amplitudes are applied.
- The shape of the distribution is similar and irrespective of the prescribed seismic input motion and consequently from the pulse characteristics. They have a minor role on the modulation of the distribution shape which is determined by the static response.

Finally, it is important to draw attention to the structure's response under seismic excitation. Specifically, inspection of the maximum and minimum principal stresses (Figure 7) helps to visualise the most vulnerable locations of the structure when a cluster of idealised Ricker pulses of different intensity trigger the model.

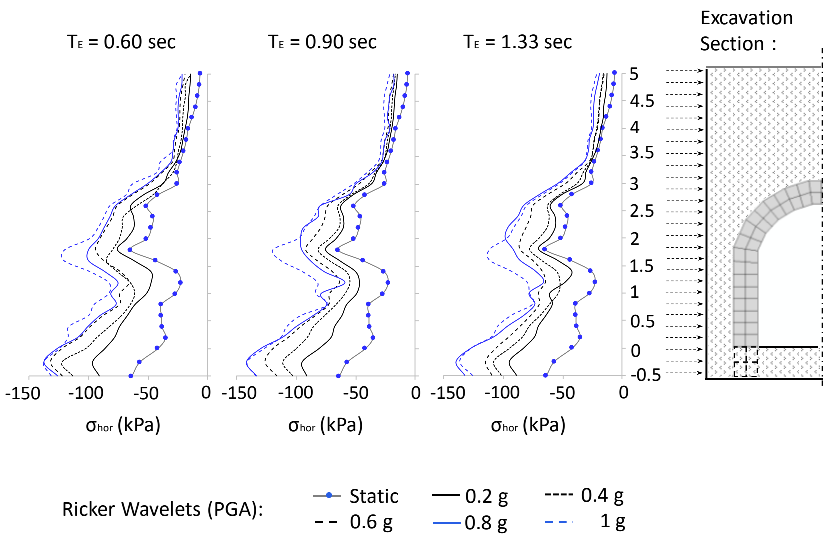

Figure 6. *Evolution of the lateral stresses that develop along the left excavation boundary when Ricker wavelets of three different durations (T_E = 0.6 s, 0.90 s, 1.33 s) are applied at the base. For each duration the structure is subjected to a wide range of acceleration amplitudes a_p from very low values (0.2 g) to moderate (0.4 g, 0.6 g) and to very strong (1 g). Distribution of the lateral stresses under static condition is also depicted.*

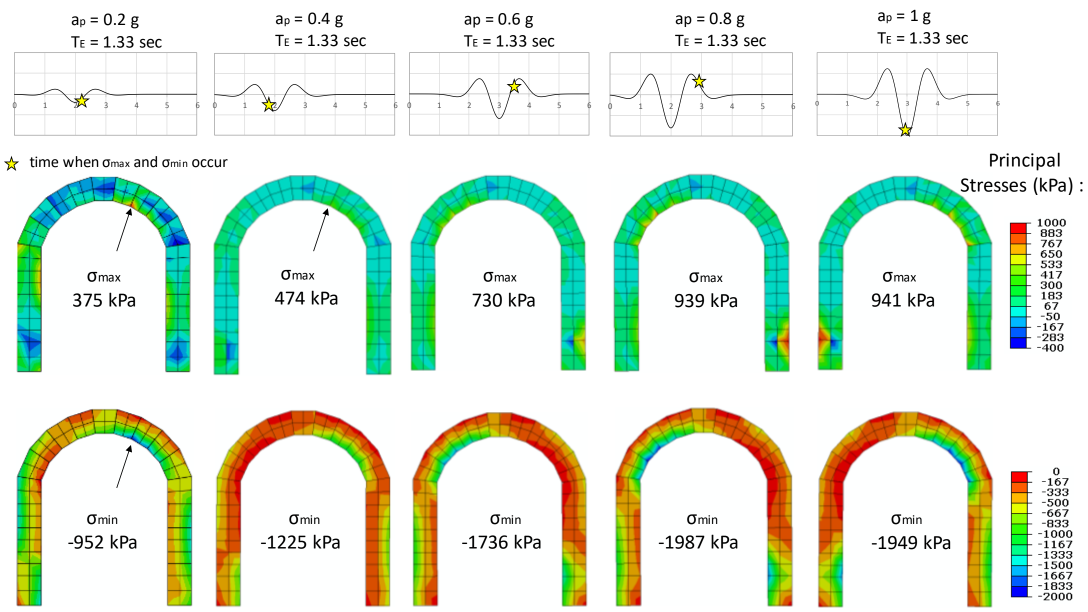

Figure 7. *Structural distress when the embedded vaulted structure is subjected to a Ricker wavelet of duration T_E = 1.33 s. For each acceleration amplitude a_p (0.2 g ÷ 1 g) contours of the maximum and minimum principal stresses are presented.*

CONCLUSIONS

The paper presents the response of an embedded vaulted tunnel into a stiff clay under vertical and lateral loading, with the aim of identifying the physical and structural mechanisms affecting the static and seismic capacity of the structure. The main findings are:

(1) A fictitious arch is developed within soil along with the structural arch to carry the overburden load. According to this 'soil arching' mechanism, stress paths are diverted within the soil around the embedded vault. The remaining part of the overburden load is sustained by the structural arch and transferred to the buttresses with a combined shear and vertical load.

(2) The backfill soil acts as a cushion for the embedded structure. It offers the horizontal reaction at the arch base to prevent arch from flattening upon the overburden load and receives directly a portion of the overburden load (soil arching).

(3) The seismic response of such structures and their vulnerability to a variety of ground motions is investigated with Ricker pulses as base excitation. The influence of the Ricker characteristics (a_p, T_E) are highlighted. For different durations T_E, different structural mechanisms are mobilised, which for high a_p may result in excessive horizontal earth reactions at different positions.

REFERENCES

Alexakis, H., Makris N. (2013). Structural stability and bearing capacity analysis of the tunnel-entrance to the stadium of ancient Nemea. Int. J. Arch. Herit. 7: 673–692.
Brandonisio, G., Angelillo, M., De Luca, A. (2020). "Seismic capacity of buttressed masonry arches." *Engineering Structures* 215 110661.
Leontari, A. (2023). Monumentic Arched Structures: Stability, Seismic Response, Soil-Structure Interaction. Dissertation, National Technical University of Athens.

Makris, N., and Alexakis, H. (2015). Limit equilibrium analysis of masonry buttresses and towers under lateral and gravity loads. Arch.Appl. Mech., 85(12), 1915–1940.